



Distance measurement by delayed optical feedback in a ring laser

L. Lombardi¹ · V. Annovazzi-Lodi¹ · G. Aromataris¹ · A. Scirè¹

Received: 22 September 2021 / Accepted: 4 March 2022 / Published online: 6 April 2022
© The Author(s) 2022, corrected publication 2022

Abstract

We numerically study the behavior of a semiconductor ring laser subject to bidirectional delayed optical feedback, when the isolated laser is in the quasi-unidirectional regime. The optical feedback, provided by two external reflectors located in front of the ring output waveguides, can modify the laser regime produced by the cross-saturation between the clockwise and the counter-clockwise mode. Thus, the system exhibits new different regimes, most of which are asymmetric and bidirectional, with alternating dominant mode. Two of these regimes are of special interest in view of applications, because the laser switching period, between the clockwise and the counter-clockwise mode, is linearly related to the time of flight from the laser to one or both reflectors. In these operating conditions, the laser is thus suitable to implement a telemeter. A convenient electrical output signal is obtained by a photodiode located behind one (partially reflecting) fixed mirror, or by measuring the voltage drop across the laser junction. Simulations are performed by mathematical models based on rate-equations, assuming typical literature parameters for a 1 mW ring laser.

Keywords Ring laser · Laser diode · Optical injection · Distance measurement

This article is part of the Topical Collection on Numerical Simulation of Optoelectronic Devices.

Guest Edited by Slawek Sujecki, Asghar Asgari, Donati Silvano, Karin Hinzer, Weida Hu, Piotr Martyniuk, Alex Walker and Pengyan Wen.

✉ V. Annovazzi-Lodi
valerio.annovazzi@unipv.it

L. Lombardi
lorenzo.lombardi@unipv.it

G. Aromataris
giuseppe.aromataris@unipv.it

A. Scirè
alessandro.scire@unipv.it

¹ Department of Electrical, Computer and Biomedical Engineering, University of Pavia, Pavia, Italy

1 Introduction

The ring laser has been proposed in the last years for different applications, ranging from the optical gyroscope (Taguki et al. 1999; Numai 2000), its main achievement, to the optical flip–flop (Trita et al. 2014) and the clock generator (Li et al. 2016).

The behavior of the ring laser has been studied both numerically and experimentally (Numai 2000; Marchal et al. 2000; Sorel et al. 2002a). Because of mode coupling due to cross-saturation, the laser exhibits bidirectional regimes, where both the clockwise (CW) and the counter-clockwise (CCW) modes are active, as well as unidirectional regimes, bistability and chaos. Also, optical feedback effects have been investigated (Friart et al. 2017), as well as methods to reduce the laser sensitivity to feedback (Khoder et al. 2018; Van Schaijk 2018; Lenstra and Schaijk 2019), or to select the laser operating wavelength and mode (Khoder et al. 2016; Vershaffelt and Khoder 2018).

Recently, we have proposed the application of a ring laser to distance measurement (Aromataris et al. 2020). In the suggested scheme, shown in Fig. 1, a laser, working in the quasi-unidirectional regime, is further subject to delayed optical feedback both from a local and from a remote mirror. Differently from most time-of-flight telemeters (Donati 2004), this instrument, which combines time-of-flight and optical injection, does not require special provisions or processing to tackle the ambiguity problem. It is very simple to implement, since, in addition to a d.c. pumped ring laser, it only requires two mirrors, and collimation or focusing optics. Also, electronic processing only consists of measuring the period or frequency of laser mode switching generated by the optical feedback in proper operating conditions.

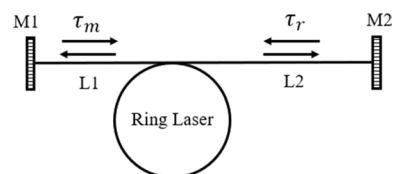
Later, Lombardi et al. (2021), we have investigated the various regimes taking place for different arm lengths (i.e., for different time of flight from laser to reflectors) in the scheme of Fig. 1. Our findings are reported in more detail in this paper.

2 Numerical model

The model used in our simulations was introduced in Aromataris et al. (2020) and is basically that of (Numai 2000) with the addition of two terms describing the optical feedback as in the Lang–Kobayashi model (Lang and Kobayashi 1980) for the standard semiconductor laser. We assume that the isolated laser (i.e., the laser without optical feedback) is in the quasi-unidirectional regime, produced by the mode cross-saturation (Sorel et al. 2002b). We will focus, in particular, on regimes in which the ring laser can be used as a telemeter, i.e., where the switching period between CW and CCW modes is linearly related to the distance of one or both reflectors from the ring laser.

In Aromataris et al. (2020), we have proposed two different equation sets, which describe the scheme of Fig. 1 with different level of accuracy. One (the three-equation model) is directly derived from that by Numai, and includes the dynamics of the carrier concentration N . In the other (the simplified two-equation model) the equation for N is adiabatically eliminated,

Fig. 1 Scheme of the semiconductor ring-laser subject to double delayed optical feedback (M1–M2: mirrors)



by the reasonable assumption that the carrier dynamics is dominated by the faster photon dynamics.

In our study, we have used both models, confirming that they are equivalent, at least in the conditions of our investigations. Most simulations have been performed with the two-equation model, which allows for faster numerical integration. The three-equation model has been used to validate the other, i.e., to confirm that the regimes investigated in detail with the fast model are indeed found also with the more complete model.

The three-equation model is shown here below for convenience:

$$\frac{dS_1}{dt} = [G - \beta S_1 - \theta S_2]S_1 - \frac{S_1}{\tau_{ph}} + \frac{\eta_2}{\tau_{in}}S_2(t - \tau_r) \quad (1)$$

$$\frac{dS_2}{dt} = [G - \beta S_2 - \theta S_1]S_2 - \frac{S_2}{\tau_{ph}} + \frac{\eta_1}{\tau_{in}}S_1(t - \tau_m) \quad (2)$$

$$\frac{dN}{dt} = \frac{J}{ed} - [G - \beta S_1 - \theta S_2]S_1 - [G - \beta S_2 - \theta S_1]S_2 - \frac{N}{\tau_n} \quad (3)$$

In these equations, S_1 , S_2 are CW and CCW photon densities, N is the carrier concentration, J is the current density, $G = G_0(N - N_0)$ is the linearized gain and G_0 is the modal gain coefficient, β and θ are the (assumed symmetrical) direct- and cross-saturation coefficients, and e is the electron charge.

The last terms of Eqs. (1) and (2) describe the optical feedback, where η_1 , η_2 account for the total attenuations from the laser to each mirror and back, τ_{in} is the round trip time in the laser cavity, and τ_r , τ_m are the round trip times from the laser to the local reflector and to the measuring mirror and back, i.e., twice the time of flight of each arm. Other symbols are listed in Table 1.

In simulations we have added noise sources, i.e., the Langevin noise (Ju et al. 2004) and the shot noise (not shown in the equations).

Photon density S can be converted into optical power P by $P = kS$, where:

Table 1 System parameters

Parameter	Description	Value
β	Self-saturation coefficient	$10^{-8} \text{ m}^3/\text{s}$
θ	Cross-saturation coefficient	$3 \times 10^{-8} \text{ m}^3/\text{s}$
$\eta_1 = \eta_2$	Reflectivity of the mirrors	0.3
τ_{ph}	Photon lifetime	2 ps
τ_n	Carrier lifetime	2 ns
N_0	Transparency carrier density	10^{24} m^{-3}
G_0	Gain coefficient	$2.5 \times 10^{-12} \text{ m}^3/\text{s}$
S_a	Active layer area	$400 \text{ }\mu\text{m}^2$
d	Active layer thickness	$0.1 \text{ }\mu\text{m}$
τ_{in}	Laser cavity round trip time	0.93 ps
v_g	Group velocity	$8.57 \times 10^7 \text{ m/s}$
S_b	Beam area	$1 \text{ }\mu\text{m}^2$
λ	Wavelength	1550 nm

$$k = h\nu v_g S_b, \tag{4}$$

h being the Plank constant, $\nu=c/\lambda$ the optical frequency (c speed of light in vacuum), while v_g and S_b are defined in Table 1.

3 Ring laser regimes

We have assumed the same parameter values (Table 1) as in Aromataris et al. (2020). These parameters are as in Numai (2000), except for adding the mirror reflections $\eta_1=\eta_2=\eta=0.3$, not present in his paper, and then selecting β and θ in order to get a laser output power of approximately 1 mW. The pump current is $I=JS_a$ 5.3 mA as in the previous paper. This working point has been chosen to obtain robust switching regimes between CW and CCW modes for all investigated arm lengths $L1, L2$.

We have found five different regimes, which are described in the following. These regimes have been observed for a variety of arm lengths. Their exact boundaries depend on the arm lengths and on the laser parameters.

To exemplify, in Fig. 2 we show the period of the ring laser switching as a function of one arm length, in the range 50 μm –45 cm, when the other is fixed to 15 cm. Since in the description of the regimes it is convenient to assume that $L1$ is the length of the shorter arm, and $L2$ is that of the longer arm, as in Fig. 1, the abscissa of Fig. 2 thus corresponds to $L1$ (shorter arm) up to 15 cm, and to $L2$ (longer arm) over 15 cm.

3.1 Regime I

An arm is very short (50 μm –2.5 mm), while the other is significantly longer (1 cm to tens of meters). In these conditions, the system exhibits an asymmetrical bidirectional regime, i.e., the CW and CCW modes are both oscillating at the same time, but with remarkably different mode amplitudes (Fig. 3). The dominant mode is alternatively CW or CCW. Switching of the dominant mode takes place periodically, with a period $T=2\tau_m$, i.e., twice the roundtrip time, or four times the time of flight, of the long arm ($L2$ in Fig. 1). This regime is described in detail in Aromataris et al. (2020). It is represented by the inset of

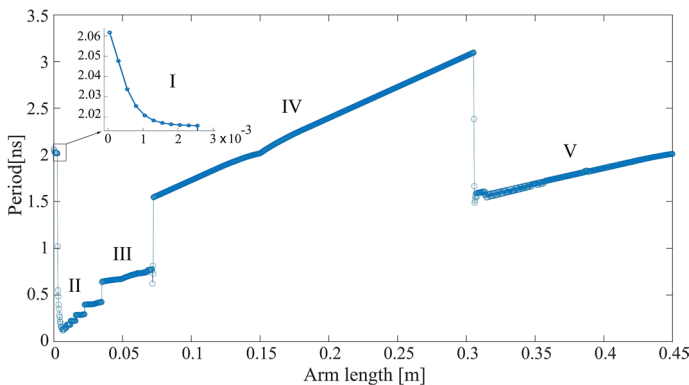


Fig. 2 Switching period as a function of one arm length, while the other arm is 15 cm, for the ring laser regimes (marked I to V) described in this paper

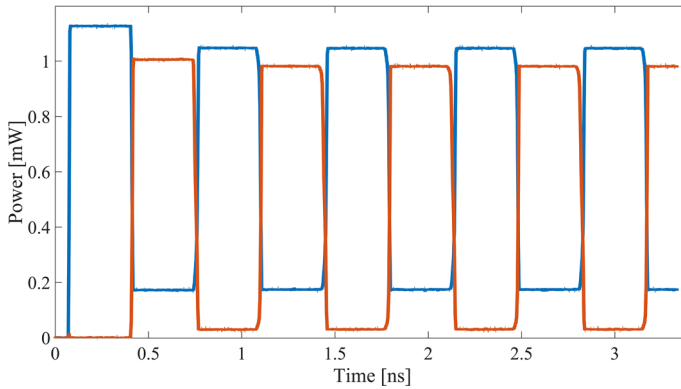


Fig. 3 Sample of power time series for CW (black, red online) and CCW (grey, blue online) modes in Regime I ($L_1 = 100 \mu\text{m}$, $L_2 = 5 \text{ cm}$)

Fig. 2, and it exhibits a small dependence on the length of the short arm (L_1 in Fig. 1). It is however characterized by a very good linearity for the measure of L_2 , as shown in Fig. 4, and it is thus suitable to make a telemeter. Provided that the condition of short (and constant) L_1 is met, $L_2 = cT/4$ (c : speed of light) with good accuracy, which increases with L_1 . For example, the error for $L_2 = 15 \text{ cm}$ is 0.8%, when $L_1 > 2 \text{ mm}$, i.e., next to the short arm maximum value for this regime (Fig. 5). We would like to point out that correcting this accuracy error requires only a scale factor and a zero-bias trimming, because the system response is remarkably linear (Fig. 6). In this regime, the system has been tested as a telemeter up to $L_2 = 32 \text{ m}$, and for different values of L_1 in the above-mentioned range.

3.2 Regime II

Both arms are relatively long (one is $> 2.5 \text{ mm}$, the other $> 1 \text{ cm}$) and their ratio is approximately in the range 0.05–0.15 with our parameter set. Also in this case, an asymmetrical bidirectional regime is found. The dynamics is complex, and, at first sight, the switching period seems nonlinearly related to the times of flight of the

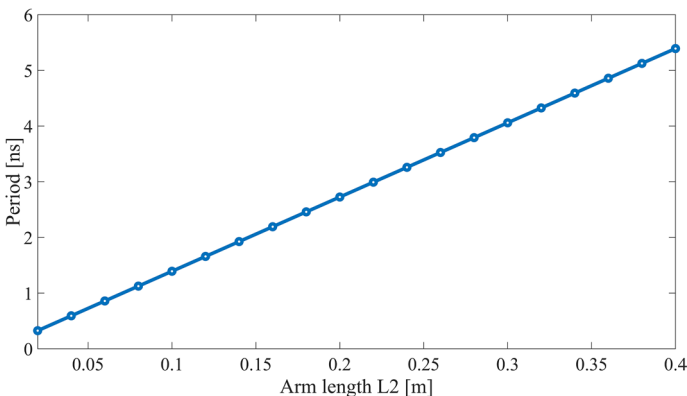


Fig. 4 Linearity plot in Regime I ($L_1 = 100 \mu\text{m}$)

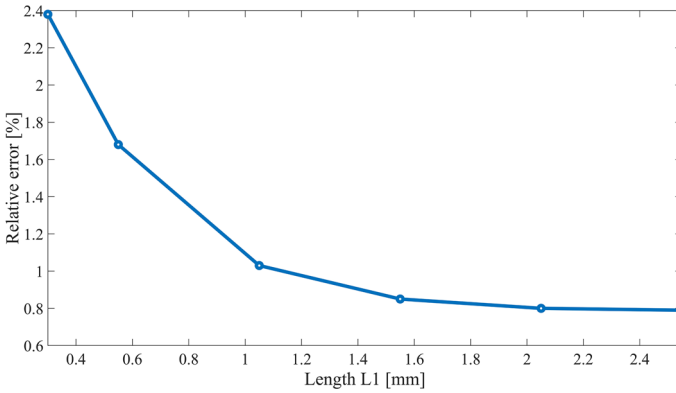


Fig. 5 Relative error in the distance measurement in Regime I ($L_2 = 15$ cm)

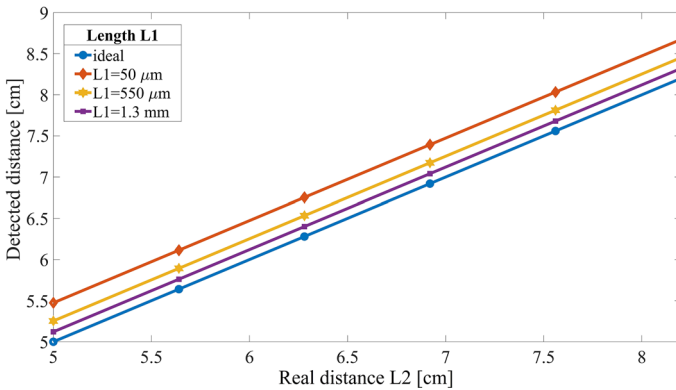


Fig. 6 Distance measured in Regime I as a function of real distance L_2 for different values of L_1 (ideal: measured distance is real distance)

two arms (Fig. 2). A more accurate analysis shows that different sub-regimes can be detected within this regime, being separated by step discontinuities. Each sub-regime exhibits an approximately linear relation of the switching period vs. the arm lengths, i.e., $T = a (\tau_r + \tau_m)$, with different slope a in the range 3–8. This regime is not suitable to make a telemeter, because of the short arm length range where each sub-regime is observed.

3.3 Regime III

Both arms are long (> 1 cm), and their ratio is larger than in the previous case (0.15–0.5 approximately, with our parameter set): this regime is still asymmetrical and bidirectional, but now the switching period is approximately the sum of the times of flight, or half the sum of the round trip times, of the two arms, i.e., $T = 0.5 (\tau_r + \tau_m)$. The linearity, however, is rather poor.

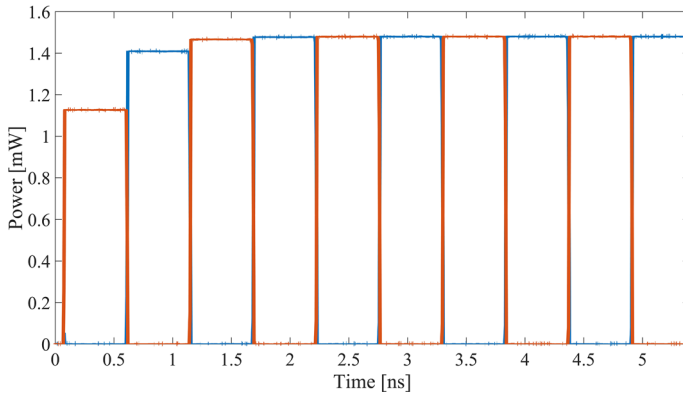


Fig. 7 Sample of power time series for CW (black, red online) and CCW (grey, blue online) modes in Regime IV ($L_1=L_2=8$ cm)

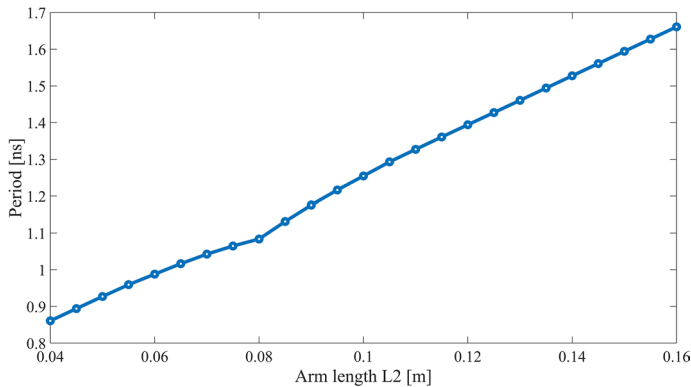


Fig. 8 Linearity plot in Regime IV ($L_1=8$ cm)

3.4 Regime IV

Both arms are long (> 1 cm) and their ratio is approximately in the range 0.5–2. In these conditions, we find an asymmetrical bidirectional regime except for $L_1=L_2$, where the laser regime is unidirectional (Fig. 7).

In both cases, the switching period is well approximated by $T=(\tau_r+\tau_m)$, i.e., the sum of the round trip times of the two arms, or twice the sum of the flight times of the two arms, and $L_1+L_2=cT/2$. This regime exhibits an approximately linear behavior (Figs. 2 and 8), and can be considered for distance measurements, even though with limited accuracy, which cannot be corrected by a simple linear scaling. It offers the possibility of measuring the distance L_1+L_2 between two moving reflectors by locating the laser approximately halfway, with a dynamic range of about 50 to 150% of the starting distance.

This regime has been experimentally demonstrated by other authors, and proposed to implement an optical flip-flop (Trita et al. 2014) and an optical clock (Li et al. 2016).

3.5 Regime V

Both arms are long (> 1 cm) but one is much longer than the other (their ratio is outside the range 0.5–2). We find several bidirectional incoming subregimes (Figs. 2 and 9), and the mean switching period T is approximately linearly related to the sum of the roundtrip times (Fig. 9), i.e., $T = a(\tau_r + \tau_m)$. However, different values of the scale constant a hold for each specific sub-regime (Fig. 9). Differently from regime II, for $L2 \gg L1$ (or $L1 \gg L2$), slope a tends to a constant value ($a \approx 0.5$, as in regime III). Nonetheless, implementing a telemeter in these conditions would be still a difficult task.

As we see in Fig. 2, the above-described regimes are separated by steep jumps of the switching period vs. the arm length curve. It is interesting to observe that these regimes are all bidirectional (but in the very special case of identical arm lengths in Regime IV) with alternating dominant modes. This means that the optical feedback provided by the two reflectors breaks the stable quasi-unidirectional regime of the isolated laser produced by the cross-saturation coefficients θ (Sorel 2002a).

As already observed, because of the linear relation holding between the switching period T and the time/times of flight, Regime I (with good accuracy) and IV (with lower accuracy) can be exploited to build a telemeter with the ring laser. This can be done, in practice, by detecting the mode power by a photodiode located behind one (semitransparent) mirror or by reading the voltage across the laser junction, and then measuring the period T of its square wave modulation, as suggested in Numai (2000) and Aromataris et al. (2020).

We would like to point out the different switching mechanism of Regime I and IV. In Regime I the period is twice the roundtrip time of the long arm only. This is the time required for the laser emission to fill and leave the longer arm. After one roundtrip time (i.e., twice the time of flight), the laser switches. The short arm fills almost immediately. However, a new commutation does not take place until the light stored in the long arm stops injecting the laser, and this requires another roundtrip time.

In Regime IV, instead, the period is the sum of the round trip times of the two arms, which means that switching between modes takes place as soon as light of one mode, travelling along one arm, reaches the laser, and starts the counter-propagating mode. This different laser behavior in different feedback conditions is not surprising, since the strong dependence of the laser regime on the feedback delay has been already observed in

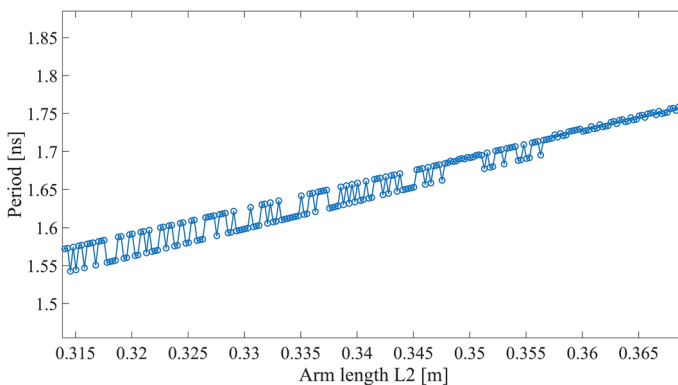


Fig. 9 Switching period as a function of $L2$ for Regime V, showing different subregimes ($L1=15$ cm)

standard lasers (Donati and Mirasso 2002). Indeed, both Regime I (Marchal et al. 2000, in somewhat different conditions), and Regime IV (Li et al. 2016; Trita et al. 2014) have been observed experimentally in ring lasers.

On the other hand, Regimes II, III and V are not well-suited for distance measurement, because the relation of the time of flight vs. the switching period is less accurate and may change between incoming sub-regimes, making this task very difficult in practice. Nevertheless, these regimes could be considered for applications where reduced linearity is not an issue. For example, they may represent an alternative to regime IV to implement an optical clock or flip-flop.

As already pointed out in Aromataris et al. (2020), the ring laser should be designed and optimized to be suitable for the proposed telemeter application. Changing the laser parameters and working point may strongly affect the system behavior because (i) the isolated laser could leave the quasi-unidirectional regime and (ii) even if the laser is in this regime, mode switching cannot take place if we substantially modify the ring laser parameters (τ_n , τ_{ph} , β , θ with respect to Table 1, or for too large attenuation η). On the other hand, the scheme of Fig. 1 is robust because (at least according to our numerical model) Regimes I and IV are found for a relatively large parameter range.

As for a practical implementation of this telemeter, we must consider that the present analysis is based on a rate equation model, which cannot take into account technological details and does not relate to a specific device.

However, as already observed, regimes I and IV can be physically explained, and experiments on Regime I and IV have been reported (Li et al. 2016; Trita et al. 2014; Marchal et al. 2000). Thus, we are confident that a telemeter based on our scheme can be successfully implemented.

A more accurate model is required to gain more insight, and get more details, on the regimes of a specific laser. Examples of technological implementations of ring lasers subject to delayed optical feedback are in (Li et al. 2016; Trita et al. 2014; Sorel et al. 2002b).

Though there is no fundamental limitation in the model as for the arm lengths, in a practical implementation a maximum operating distance is expected, due to available power and beam attenuation, also depending on focusing or collimating optics. Moreover, with a real device, the details of laser switching dynamics are expected to play a role. Typical expected switching times are of the order of 1.5 ns with a spread of 0.7% to 0.001%, depending on the feedback level (Li et al. 2016). This fluctuation would affect the telemeter accuracy on a single round trip. Since in our scheme we measure the switching frequency or period, a mean over different flight times is intrinsically performed, and the effect of fluctuations on the switching time is reduced. In a typical pulse time-of-flight telemeter the same result is obtained by taking the mean over several single measurements.

4 Conclusions

In this paper we have numerically investigated the regimes of a ring laser subject to delayed optical feedback from two reflectors, when the isolated laser is in the quasi-unidirectional regime. By rate equation models, we have found two regimes that are suitable for the design of a time-of-flight telemeter based on a properly designed ring laser, with different levels of accuracy. This scheme has a very simple optical arrangement, requiring only collimation or focalization of the laser emission, while electronic processing simply consists

in photodetection and amplification of the laser emission, and in measuring the period or frequency of the square wave output signal.

Author contributions All authors contributed to the study conception and design. Code preparation was performed by AS, LL and GA. The first draft of the manuscript was written by VA-L and all authors commented on previous versions of the manuscript. All authors read and approved the final manuscript.

Funding Open access funding provided by Università degli Studi di Pavia within the CRUI-CARE Agreement. This work was funded by the Department of Electrical, Computer and Biomedical Engineering of the University of Pavia, Pavia, Italy.

Data availability All relevant data generated or analysed during this study are included in this published article.

Code availability Custom code developed in Matlab is available on request.

Declarations

Conflict of interest The authors declare that they have no conflict of interest.

Open Access This article is licensed under a Creative Commons Attribution 4.0 International License, which permits use, sharing, adaptation, distribution and reproduction in any medium or format, as long as you give appropriate credit to the original author(s) and the source, provide a link to the Creative Commons licence, and indicate if changes were made. The images or other third party material in this article are included in the article's Creative Commons licence, unless indicated otherwise in a credit line to the material. If material is not included in the article's Creative Commons licence and your intended use is not permitted by statutory regulation or exceeds the permitted use, you will need to obtain permission directly from the copyright holder. To view a copy of this licence, visit <http://creativecommons.org/licenses/by/4.0/>.

References

- Aromataris, G., Lombardi, L., Sciré, A., Annovazzi-Lodi, V.: Time-of-flight telemeter based on a ring laser. *Opt. Quant. Electron.* **52**, 398 (2020)
- Donati, S.: Electro-optical instrumentation, Section 3. Prentice Hall, Prentice Hall (2004)
- Donati, S., Mirasso, C.: Feature section on optical chaos and applications to cryptography. *Journal of Quantum Electronics* **38**(9), 1137–1196 (2002)
- Friart, G., et al.: Stability of steady and periodic states through the bifurcation bridge mechanism in semiconductor ring lasers subject to optical feedback. *Opt. Express* **25**(1), 339–350 (2017)
- Ju, R., Spencer, P.S., Shore, K.A.: The relative intensity noise of a semiconductor laser subject to strong coherent optical feedback. *J. Opt.* **8**, S775–S779 (2004)
- Khoder, M., Van der Sande, G., Danckaert, J.: Effect of external optical feedback on tunable micro-ring lasers using on-chip filtered feedback. *IEEE Photonic Technol. Lett.* **28**(9), 959–962 (2016)
- Khoder, M., Van der Sande, G., Vershaffelt, G.: Reducing the sensitivity of semiconductor ring lasers to external optical injection using selective optical feedback. *J. Appl. Phys.* **124**, 133101 (2018)
- Lang, R., Kobayashi, K.: External optical feedback effects on semiconductor injection laser properties. *IEEE J. Quantum Electron.* **16**, 347–355 (1980)
- Lenstra, D., van Schaijk, T.T.M.: Toward a feedback-insensitive semiconductor laser. *IEEE J. Sel. Top. Quantum Electron.* **25**(6), 1502113 (2019)
- Li, S., et al.: Square-wave oscillations in a semiconductor ring laser subject to counter-directional delayed mutual feedback. *Opt. Lett.* **41**(4), 812–815 (2016)
- Lombardi, L., Annovazzi-Lodi, V., Aromataris, G., Sciré, A.: Optical feedback regimes suitable for distance measurement with a ring laser. In: Proceedings of NUSOD 2021, 21st International Conference on Numerical Simulation of Optoelectronic Devices, pp. 89–90. IEEE, Torino (2021)

- Marchal, L., et al.: Square-wave oscillations in semiconductor ring lasers with delayed optical feedback. *Opt. Express* **20**(20), 1161–1167 (2000)
- Numai, T.: Analysis of signal voltage in a semiconductor ring laser gyro. *J. Quantum Electron.* **36**(10), 1161–1167 (2000)
- Sorel, M., Laybourn, J.R., Giuliani, G., Donati, S.: Unidirectional bistability in semiconductor waveguide ring lasers. *Appl. Phys. Lett.* **80**(17), 3051–3053 (2002a)
- Sorel, M., et al.: Alternate oscillations in semiconductor ring lasers. *Opt. Lett.* **27**(22), 1992–1994 (2002b)
- Taguchi, K., Fukushima, K., Ishitani, A., Ikeda, M.: Experimental investigation of a semiconductor ring laser as an optical gyroscope. *Trans. Instrum. Meas.* **48**(6), 1314–1318 (1999)
- Trita, A., Mezosi, G., Sorel, M., Giuliani, G.: All-optical toggle flip–flop based on monolithic semiconductor ring laser. *Photonics Technol. Lett.* **26**(1), 96–99 (2014)
- Van Schaijk, T.T.M., Lenstra, D., Bente, E., Williams, K.A.: Theoretical analysis of a feedback insensitive semiconductor laser using weak intracavity isolation. *IEEE J. Sel. Top Quantum Electron.* **24**(1), 1800108 (2018)
- Verschaffelt, G., Khoder, M.: Directional power distribution and mode selection in micro ring lasers by controlling the phase and strength of filtered optical feedback. *Opt. Express* **26**(11), 14315–14328 (2018)

Publisher's Note Springer Nature remains neutral with regard to jurisdictional claims in published maps and institutional affiliations.